



Restratification by Mixed Layer Instabilities

Baylor Fox-Kemper and Raffaele Ferrari

MIT Earth, Atmospheric and Planetary Sciences Dept. and NOAA Climate and Global Change Program
MIT 54-1410, 77 Mass. Ave., Cambridge, MA 02139, baylor@alum.mit.edu

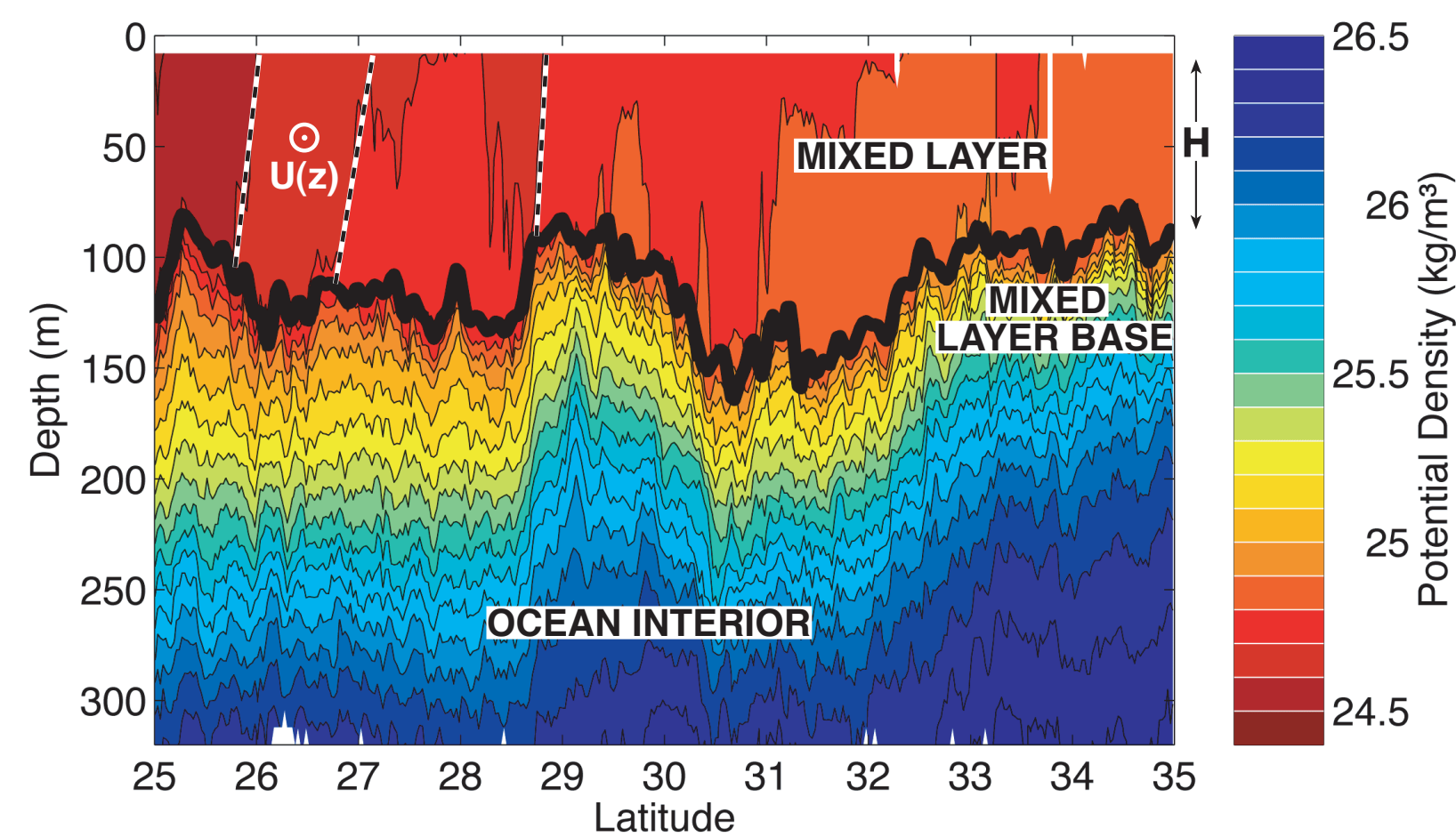
The Geophysical Turbulence Program Workshop on
Coherent Structures in Atmosphere and Ocean



I. Abstract

We study the restratification of the oceanic surface mixed layer that results from lateral inhomogeneities in the surface density field. Mixed layer models are quite successful at reproducing the deepening of the mixed layer, but the restratification phase is not as well understood and model bias is especially large when there are horizontal variations in the density field. These lateral inhomogeneities give way to ageostrophic baroclinic instabilities which slump the horizontal density gradients under the effect of rotation. These mixed-layer instabilities (MLI) differ from ocean interior instabilities because of the weak surface stratification, and the fact that their lower 'boundary' is a density jump in the transition layer between the mixed layer and the ocean interior. Spatial scales are $O(1-10)$ km and growth rates are faster than a day. We use both linear stability analysis and fully nonlinear simulations to study the impact of MLI on mixed layer restratification. Finally we discuss the issue of parameterization of MLI-driven restratification in mixed layer models.

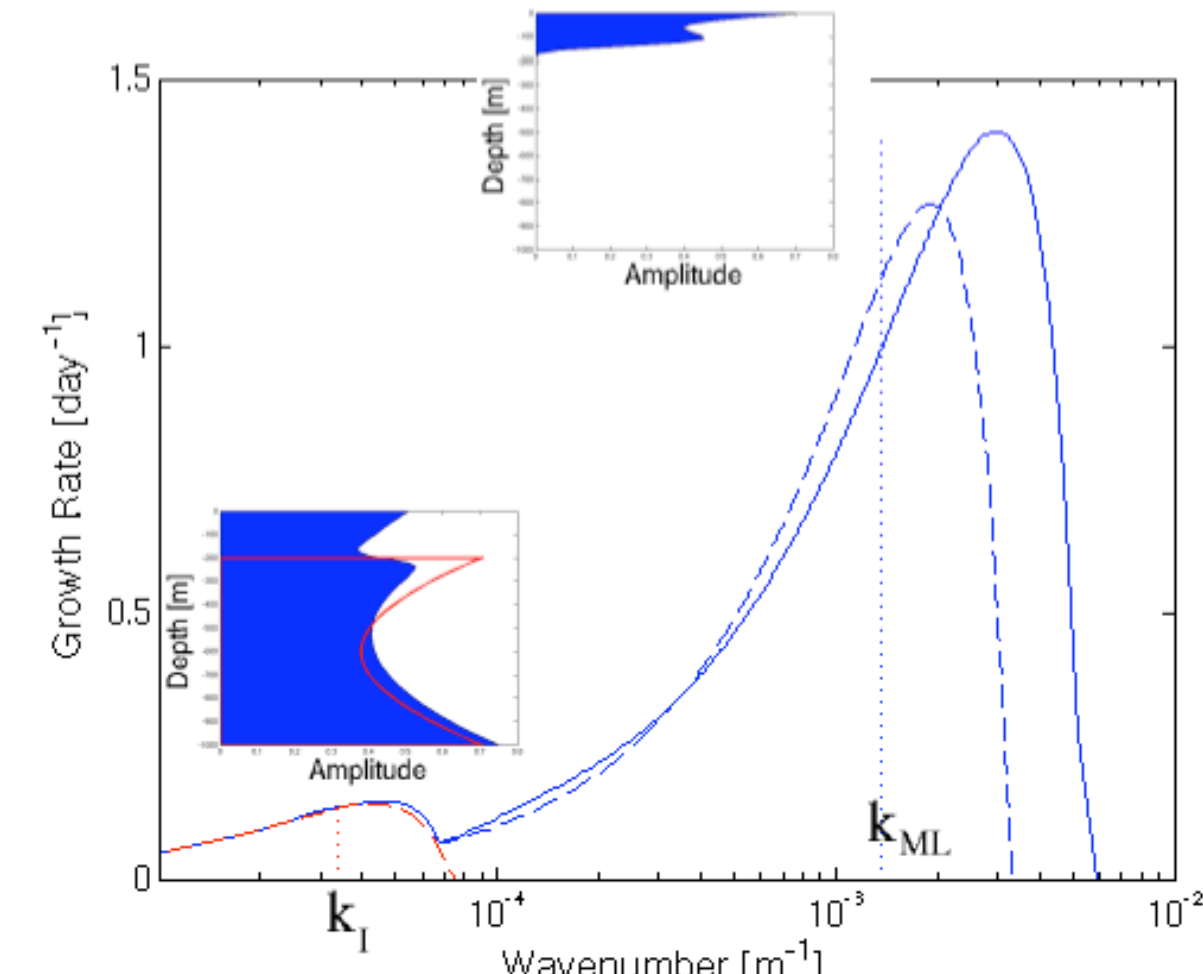
II. Ocean Mixed Layer



Potential density section from towing a CTD following a sawtooth pattern in the Subtropical Gyre of the North Pacific between 25N and 35N at 140W. (Ferrari and Rudnick, 2000).

The ocean mixed layer (ML) is a layer of weak stratification in the upper 100 m overlying the more stratified thermocline. The ML is not horizontally homogeneous: there are numerous lateral density gradients. ADCP measurements collected during the same campaign confirm that the lateral density gradients are in geostrophic balance with a sheared velocity U_z as schematized here.

III. Mesoscale vs. Mixed Layer Instabilities



The linear instability of the upper 1000m of the ocean water column: a 200m deep ML with $N \approx 4 \times 10^{-4} s^{-1}$, $U_z = 2 \times 10^{-4} s^{-1}$, and $Ri = 3.6$ sits on a 800m thermocline with $N \approx 4 \times 10^{-3} s^{-1}$, $U_z = 2 \times 10^{-4} s^{-1}$ and $Ri = 360$. For comparison, shown in red is the instability of the 800m ocean interior alone with a rigid lid replacing the ML. Also shown are the inverse deformation radii and the fastest-growing modes of the ML and interior (inset). (solid = quasi-geostrophic, dashed = Stone (1971) ageostrophic estimate).

The baroclinic instability of the upper ocean water column is dominated by two distinct modes: interior instabilities with fastest-growing wavelengths close to the internal deformation radius (≈ 60 km) and mixed-layer instabilities (MLI) with growth peaking near the ML deformation radius (≈ 1.5 km). The former span the whole ocean depth. MLI are confined to the ML.

MLI and interior modes roughly agree with the Eady (1949) model. They possess exponential edge waves trapped to the top and bottom of their domain. When these edge waves interact, linear instability results. They both extract energy from horizontal density gradients, resulting in restratification.

The fastest-growing baroclinic instability is near the deformation radius: k_{ML} (for MLI) or k_I .

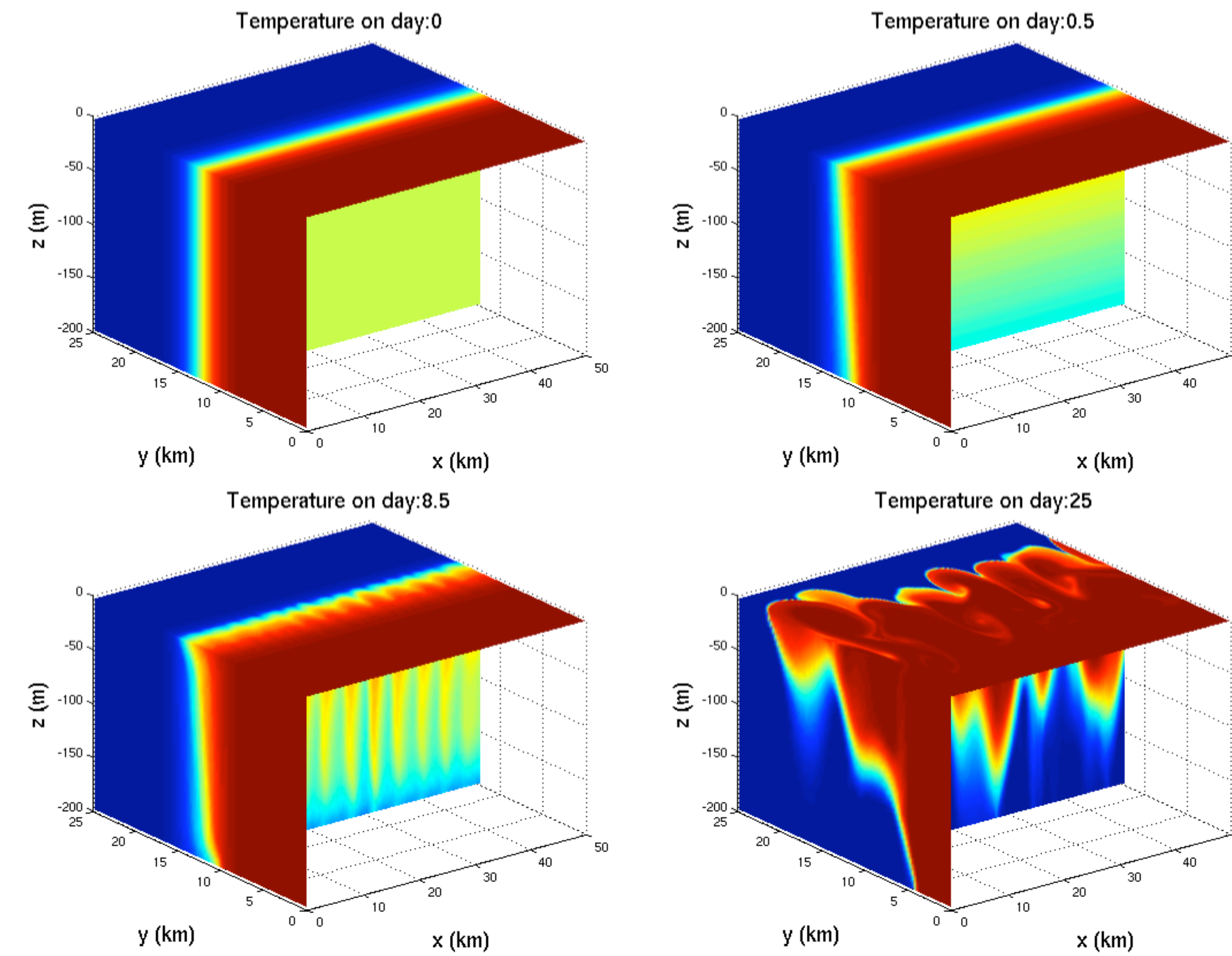
$$O(1) = \frac{k^2}{k_{def}^2} = \frac{1}{L^2} \frac{N^2 H^2}{f^2} = \frac{U^2}{f^2 L^2} \frac{N^2 H^2}{U^2} = Ro^2 Ri \quad (1)$$

The interior ocean has large Ri , so interior instabilities have small Ro and are a quasi-geostrophic baroclinic instability (Eady, 1949). The MLI, on the other hand, occur where $Ri=O(1)$, so have $Ro=O(1)$, and are an ageostrophic baroclinic instability (Stone, 1971).

Mixed layer instabilities (MLI) differ notably from those in the thermocline because of the weak stratification and the presence of a moving interface at their base. A linearized ML dynamics that includes a moving bottom boundary reveals that a tilting base provides a topographic- β -like effect and gives a low wavenumber cutoff. Thus, the MLI occur only at wavelengths near the ML deformation radius.

IV. Development of Mixed Layer Eddies

Finite-amplitude, nonlinear aspects of MLI development allow the direct study of eddy mixing and restratification rates that may be utilized in parameterizations. We consider the Rossby adjustment of initially-vertical density surfaces in a $200m \times 25km \times 50km$ channel (representing a section of the ML after the passage of a storm or isolated convective event):



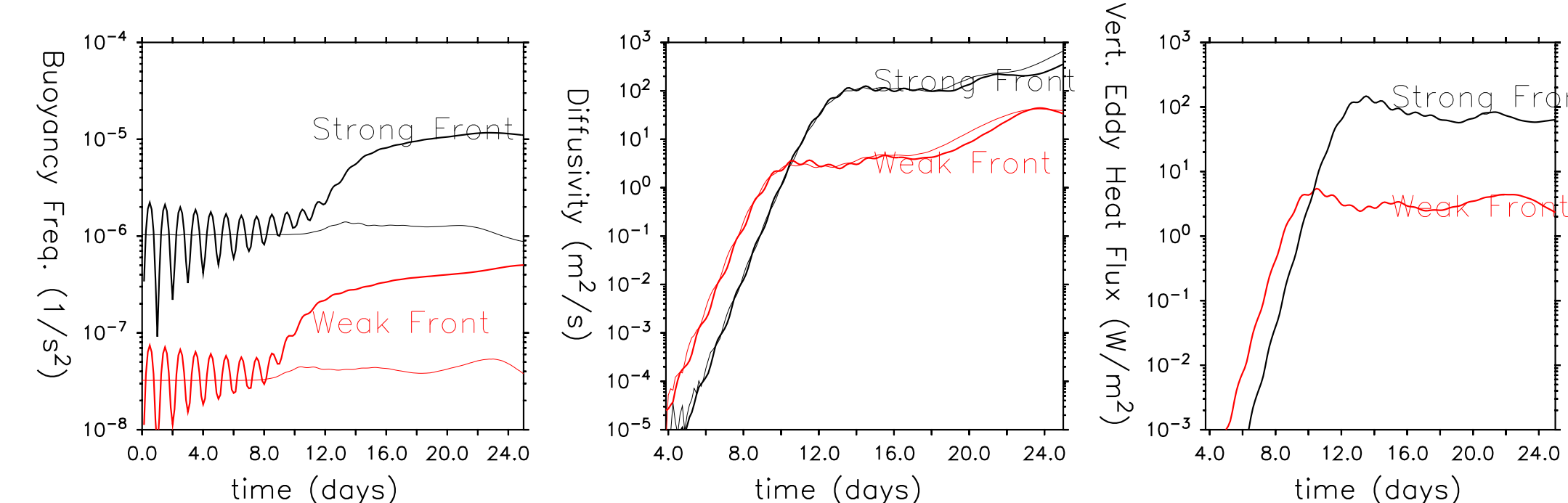
Snapshots of Rossby adjustment and instability. Total density difference: 0.008 kg/m^3 .

Initially, the density surfaces drop gravitationally into an inertial oscillation about the state where $\rho_z f / \rho_y^2 \approx Ri \approx 1$. This stage of the adjustment is detailed by Tandon and Garrett (1994) and Ou (1984). The first two snapshots show the range of this oscillation in our simulation.

However, this oscillating state is not stable to MLI. Initially they grow as Eady (1949)-like waves much as predicted by the preceding analysis and with the ageostrophic growth rates due to Stone (1971). Day 8.5 above shows these waves nicely. The waves extract available potential energy from the mean stratification and drive a slumping/restratification of the initial front.

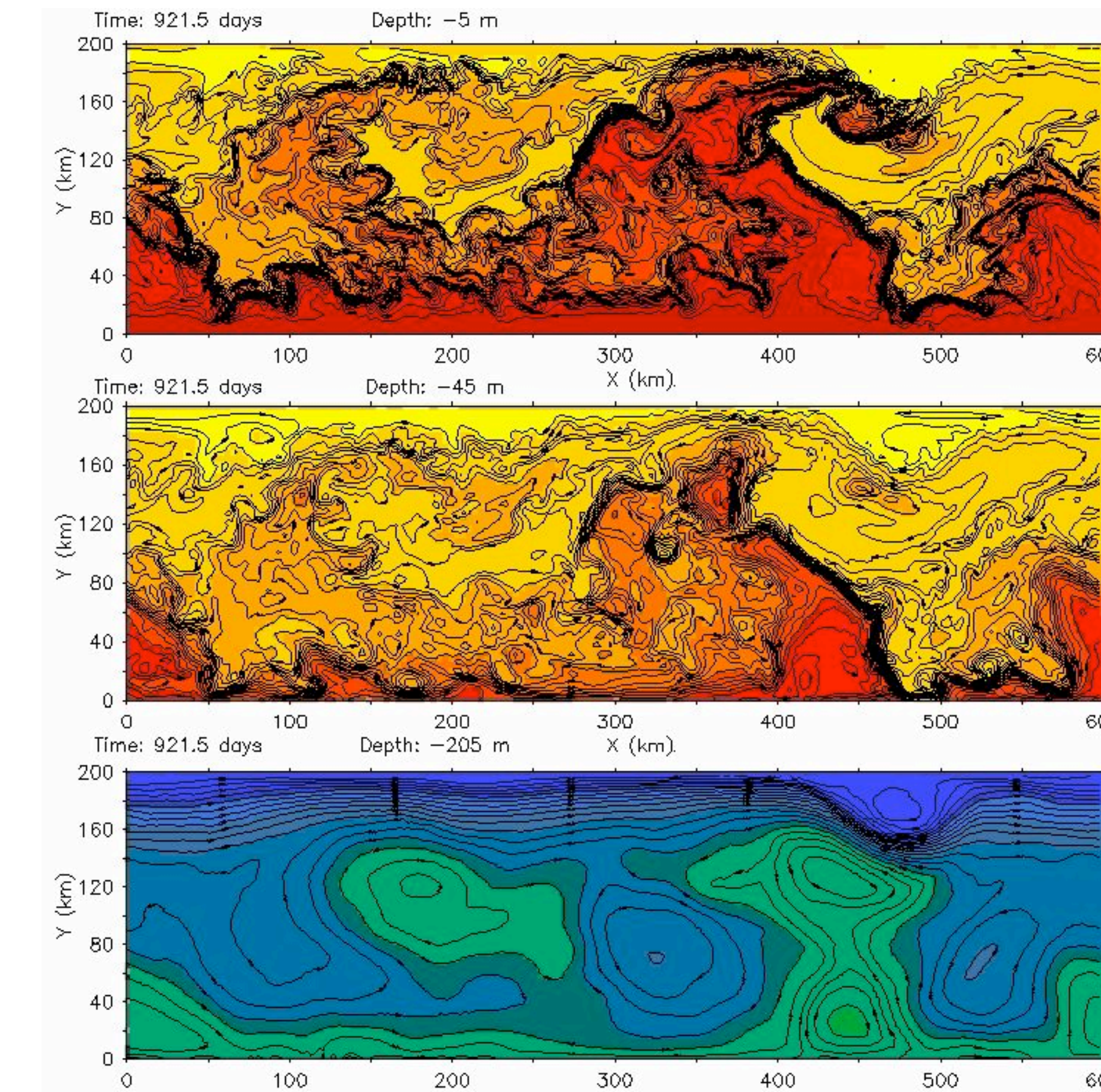
The restratification is enhanced as the waves reach finite amplitude and begin to nonlinearly interact strongly. The fully nonlinear waves are shown at day 25 above. Note that their length-scale has increased dramatically, as expected from an inverse energy cascade.

The following figure shows the restratification process for a weak front ($0.1K/10km$) and a strong front ($0.5K/10km$). Note the initial inertial oscillations and the significantly stronger restratification that occurs as the MLI develop. The effect of restratification by MLI may be parameterized by a Gent and McWilliams (1990) parameterization. However unlike in the ocean interior where a diffusivity of $O(1000 \text{ m}^2/s)$ is appropriate, we see that for MLI, $O(10-100 \text{ m}^2/s)$ is better. Previous attempts to use Gent and McWilliams (1990) too rapidly restratified the ML, but they used interior values of Gent-McWilliams diffusivity rather than MLI diffusivity values. Still, the implied magnitude of MLI's vertical eddy heat flux is significant compared to other mixed layer processes (e.g., diurnal-average surface fluxes and entrainment $O(100)W/m^2$).



Eddy statistics from two nonlinear calculations with different initial front strength.

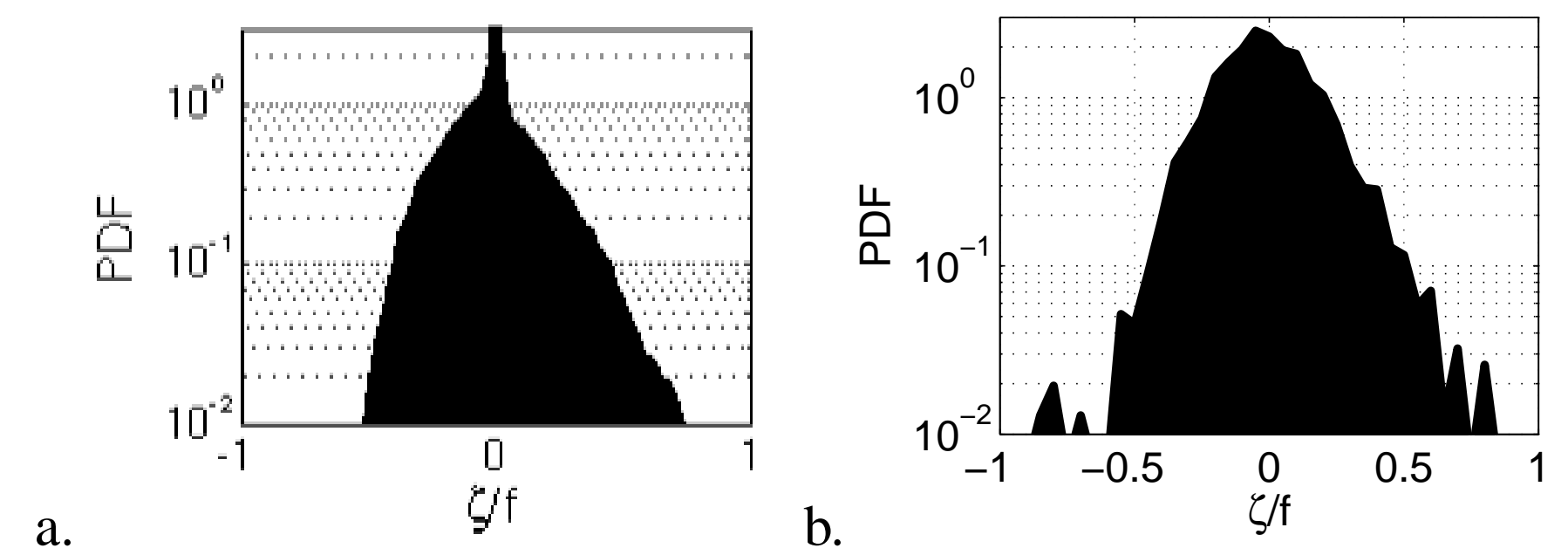
VI. ML Eddies Interact with Mesoscale and Mixing



Snapshot of temperature from a channel flow in x-direction with buoyancy restored near sidewalls at $y=0$ and 200 km to create a current subject to mesoscale baroclinic instability. A no-net diurnal cycle of heating/cooling at the surface maintains a 100m-deep surface mixed layer by nightly convection. The interior flow shows a rich mesoscale eddy field (bottom panel). In the ML, MLI form along the fronts caused by the straining of surface temperature gradients from the mesoscale eddies below (upper 2 panels). After nightly mixing and frontogenesis, the MLI rapidly restratify the ML.

VI. Strong ML Eddies in Observations

Munk and Armi (2001) have recently noted the ubiquity of $O(1-10)$ km spirals of surfactant on the ocean surface. These spirals have a preferentially cyclonic rotation, and are often seen after long periods of hot weather. We note that the preferentially-cyclonic eddies formed by MLI in our nonlinear Rossby adjustment share these features, and share the preference for cyclonic rotation to a realistic degree (see figure below). Ultimately, this can be attributed to the conservation of initially-vanishing potential vorticity.



Probability density function of relative vorticity divided by Coriolis parameter. (a) The numerical simulation at day 25, and (b) ADCP measurements in the North Pacific (Rudnick, 2001).

VI. Conclusions

- MLI are ubiquitous in MLI-permitted models and observations with lateral variations in ML density.
- They are small in scale $O(1-10km)$ and fast-growing $O(\leq 1 \text{ day})$.
- They are ageostrophic and are limited to wavelengths near the ML Rossby radius.
- They do a large share of the restratification for $Ri > 1$.
- They are parameterizable via a Gent and McWilliams diffusivity $O(10 - 100 \text{ m}^2/s)$.
- Look for Boccaletti et al. (2005)!

References

Boccaletti, G., R. Ferrari, and B. Fox-Kemper: 2005, Mixed layer instabilities. Submitted.
Eady, E. T.: 1949, Long waves and cyclone waves. *Tellus*, **1**, 33-52.
Ferrari, R. and D. Rudnick: 2000, The thermocline structure of the upper ocean. *Journal of Geophysical Research*, **105**, 16,857-16,883.
Gent, P. R. and J. C. McWilliams: 1990, Isopycnal mixing in ocean circulation models. *Journal of Physical Oceanography*, **20**, 150-155.
Munk, W. and L. Armi: 2001, Spirals on the sea: A manifestation of upper-ocean stirring. *Proceedings of the 12th 'Aha Huiho' a Hawaiian Winter Workshop*.
Ou, H.: 1984, Geostrophic adjustment: A mechanism for frontogenesis? *Journal of Physical Oceanography*, **14**.
Rudnick, D.: 2001, On the skewness of vorticity in the upper ocean. *Geophysical Research Letters*, **28**.
Stone, P. H.: 1971, Baroclinic stability under non-hydrostatic conditions. *Journal of Fluid Mechanics*, **45**.
Tandon, A. and C. Garrett: 1994, Mixed layer restratification due to a horizontal density gradient. *Journal of Physical Oceanography*, **24**.